The Design and Fabrication of Monomode Optical Fiber

B. JAMES AINSLIE, KEITH J. BEALES, CLIVE R. DAY, AND JAMES D. RUSH

Abstract—**The design of monomode fibers is discussed in the context of optimizing fiber loss and dispersion simultaneously, with reference to the materials choices and limitations to preform and fiber fabrication by the MCVD technique. Two classes of monomode structure—matched cladding and depressed cladding—are considered. Ultralow attenuation has been achieved reproducibily in both classes of fiber. The control of fiber geometry and dispersion is also discussed. Matched cladding fiber suitable for systems operating at both 1.3 and 1.55 μm has been studied and mean losses of 0.45 dB/km at 1.3 μm and 0.28 dB/km at 1.55 μm have been achieved for a total of 130 km. The behavior of depressed cladding fiber is compared with predictions from the theory of propagation in *W* fibers. Depressed cladding fiber with stable guidance has been demonstrated with attenuation of 0.37 dB/km at 1.3 μm and 0.21 dB/km at 1.55 μm.**

I. Introduction

VERY low attenuation has been achieved in graded index multimode fiber during the last few years (e.g., <1 dB/km in the wavelength range 1.2-1.6 μm [1]), but even lower losses have been found in monomode fibers and the announcement in 1979 of fiber with an attenuation of 0.2 dB/km at 1.55 μm [2] suggested that systems could be made with repeater spacings of 50-100 km.

The bandwidth available in multimode fibers tends to be limited by the modal dispersion arising from errors in the refractive index profile, and typical high quality graded index fibers show measured bandwidths of ~1 GHz · km [3]. Monomode fibers of the type described in [2] have very low dispersion at 1.3 μm, and hence extremely high bandwidths (>100 GHz · km) are possible in this transmission window. Theoretical calculations have also shown that the wavelength of minimum dispersion (λ_0) in germania doped silica monomode fibers may be adjusted to lie in the broader transmission window centered at 1.55 μm [4]. This may be achieved by intentionally increasing the waveguide dispersion to balance the materials dispersion at wavelengths >1.3 μm, since they are of opposite signs. In practice, however, shifting λ_0 from ~1.3 to ~1.55 μm generates other problems since it entails reducing the fiber core diameter $2a$ from 8-10 μm to 4-5 μm, while increasing the refractive index difference δn between core and cladding from ~0.003 to > 0.01. This requires the GeO_2 content in the core of the fiber to be increased significantly, which can lead to substantial excess losses [5].

We have been studying the design of monomode fibers in terms of optimizing the loss and bandwidth required to make high capacity systems over long unrepeatered distances, and we consider the implications of fiber design for practical fiber performance. Fibers have been produced by the MCVD technique, which is widely used and well documented [1], but here we highlight features which we have developed to improve fiber performance. Two classes of fiber have been investigated: those with matched claddings in which the refractive index of the deposited cladding is adjusted to equal that of the substrate, and those with depressed claddings in which the refractive index of the cladding is reduced below that of the substrate. A range of fiber designs is considered for both classes of fiber, and the compromises between achieving low optical loss and dispersion shifting are investigated.

The behavior of practical monomode fibers with depressed claddings is compared with that expected from the propagation theory for *W* fibers [6]. The use of fibers of optimized design in laboratory demonstration systems is described, and the results of our studies are summarized in the context of their implications for possible fiber systems.

II. Background and Fiber Fabrication

The ultra-low-loss monomode fiber reported originally by Miya *et al.* [2] comprised a core of GeO_2-SiO_2 glass with a deposited cladding of pure SiO_2 (regions 1 and 2, respectively, in Fig. 1). This structure requires very high process temperatures to sinter the SiO_2 particles in the MCVD process to form clear homogenous layers, and in monomode fiber the deposited cladding occupies typically 25-50 times the volume of the core, as will be discussed later in detail. This means that only relatively small preforms can be made without severe distortion of the substrate tube. One possible solution to this problem is to pressurize the tube during deposition [7], but this can prove difficult to control in practice, and an alternative method is to dope the deposited cladding with additives which lower the deposition temperature [8]. Phosphorus makes an excellent dopant in this respect since 1-2 percent P_2O_5 in SiO_2 lowers the deposition temperature by ~200° C, but there are undesirable side effects. One is that P_2O_5 raises the refractive index of the cladding, which creates a secondary waveguide with respect to the substrate. In an attempt to alleviate this problem some workers have used a low concentration (~0.1 percent) of P_2O_5 in the cladding and claim that the secondary waveguide effects are so weak that they are not important over long lengths of fiber [9]. Our approach, however, has been to maximize the benefits of low process temperature by using 1-2 percent P_2O_5 and then cancelling the increase in refractive index by introducing a second dopant which depresses the refractive index to the level of the substrate [10]. Although

Manuscript received September 14, 1981; revised December 8, 1981.
The authors are with British Telecom Research Laboratories, Ipswich, Suffolk, England.

0018-9480/82/0400-0360$00.75

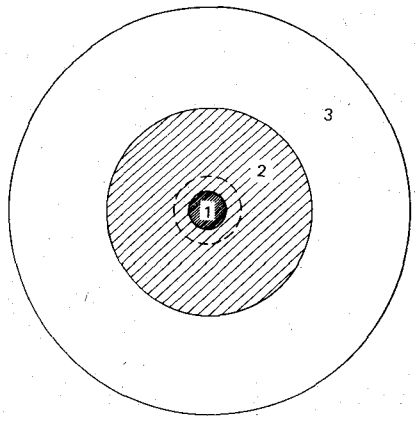

Fig. 1. Schematic cross section of monomode optical fiber, showing: 1, core (radius a), 2, deposited cladding, and 3, silica substrate. The dashed circle in region 2 at radius $r \sim 2a$ represents the limit of the graded inner cladding.

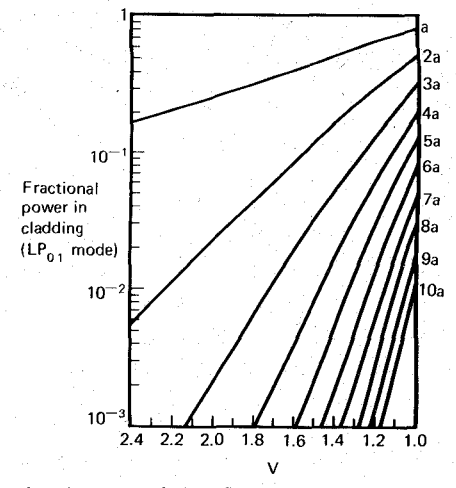

Fig. 2. Fractional power of the LP_{01} mode at various multiples of the core radius a, as a function of the normalized frequency $V = 2\pi a (n_1 - n_2)^{1/2}/\lambda$, where n_1 and n_2 are the respective refractive indices of core and cladding and λ the wavelength. Only the LP_{01} mode propagates for $V < 2.4$.

B_2O_3 and F are suitable dopants, F is preferred since it allows low transmission loss over the wavelength range 1-1.8 μm to be achieved, whereas with B_2O_3, the IR absorption edge limits operation to wavelengths <1.3 μm. A second drawback with P_2O_5 is the broad absorption peak at ~ 1.6 μm due to the P-OH first overtone at this wavelength [11]. There is also some evidence that the high energy tail of the P-O infrared absorption may contribute to the loss in the long wavelength region [12], but Irven has indicated that P-OH is the dominant effect for this type of fiber [13].

In monomode fiber an appreciable fraction of the power propagates in the cladding, and Fig. 2 shows the fraction of total guided power which travels outside a given radius in the fiber as a function of the normalized frequency V. These curves were calculated from Gloge's approximations for monomode fiber [14], and show that although 20-40 percent of the power travels in the cladding for a typical range of V, at two core radii from the center only 1-5 percent remains. In a monomode fiber designed to operate at 1.3 and 1.55 μm ("dual window" fiber), the LP_{11} mode cutoff will lie in the range 1.1-1.25 μm and consequently V will be ~ 1.8 at 1.6 μm. Thus, maintaining a low P_2O_5 concentration in the annulus $a < r < 2a$ (shown dotted in Fig. 1) should greatly assist in limiting any excess loss due to P_2O_5. A pure SiO_2 inner cladding region has previously been reported [10], but this still requires a high process temperature. In this work we have developed the graded inner cladding shown in Fig. 3, which allows the average process temperature to be lower for the inner cladding while minimizing the drawbacks of P_2O_5 in a region where the guided power is still at a high level.

Fig. 3(a) shows a refractive index profile measured in a typical monomode preform using a commercially available instrument [15]. The oscillations in the refractive index reflect the gradation of dopant in each traverse caused by evaporation and composition-dependent layering effects in the MVCD process [16]. Fig. 3(b) is a schematic representation of Fig. 3(a) showing the P_2O_5 +F doped outer cladding, the graded inner cladding, and the GeO_2-doped core. The concentration of P_2O_5 +F is reduced over several passes from radius $2a$ to radius a to optimize ease of fabrication and loss. Fig. 3(a) also shows the central depression in refractive index

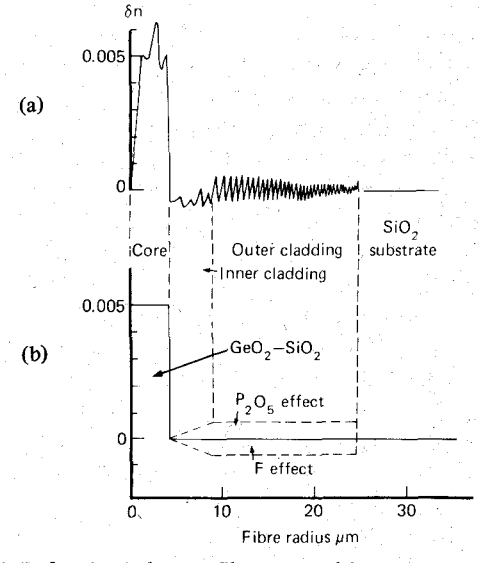

Fig. 3. (a) Refractive index profile measured in a monomode preform showing central depression in refractive index and structure due to evaporation and composition dependent layering effects in the MCVD process. (b) Schematic refractive index profile showing the effects of P_2O_5 and F and the graded inner cladding.

which occurs in the MCVD process and results from evaporation of GeO_2 during the collapse of the structure to form the preform rod (requiring a temperature $\sim 300°C$ higher than for deposition). This depression can be avoided by keeping $GeCl_4$ in the oxygen carrier gas during collapse. In addition to the advantages described above, the graded inner cladding means that there is a low concentration of F at $r = a$. SEM scans of fibers and preforms show that F can diffuse for a distance $\sim a$ at typical process temperatures [17], so a low concentration of F helps to maintain a sharp gradient in refractive index at the core-cladding boundary.

Fig. 2 also illustrates the requirement for the radius of the deposited cladding b to be at least $5a$. For example, at $V = 1.6$ about 0.1 percent of the power travels in the region $r > 5a$, and V-values of this order represent the practical limit of

operation before bending losses become appreciable in typical fibers. Power traveling in the substrate will suffer rapid attenuation due to the relatively high concentration of metallic impurities and water in this material. Other workers have also shown that $b/a > 5$ is necessary to ensure that excessive loss is not caused by diffusion of OH from the substrate into the guiding region in fibers with pure SiO_2 claddings [9].

In this work the high purity raw materials (Merck Optipur) have not been further purified, but the oxygen carrier gas is passed over heated platinized alumina pellets to convert any hydrocarbon impurities which may be present to H_2O and CO_2, and the gas is dried using freshly baked molecular sieves at high pressure. The deposition tubes were Heralux WG in sizes 20 X 16 mm and 25 X 19 mm, and deposition rates were in the range 0.25-0.75 g/min for the cladding and 0.05-0.1 g/min for the core. In early fibers the OH peak at 1.39 μm was measured to be 10-20 dB/km, from which an OH concentration of ~0.2 parts in 10^6 was inferred. The collapse stage of the preform fabrication is particularly critical in monomode fibers since the guided power is concentrated in the last few deposited layers. During deposition the decomposition of the halide raw materials liberates free chlorine, which reacts strongly with any residual OH to form HCl, which is volatile and not incorporated into the glass structure. However, if the substrate tube is collapsed with only an atmosphere of the O_2 carrier gas present then residual water can react with the exposed inner layers, increasing the OH content of the guiding region. 1% Cl_2 was therefore introduced into the O_2 at this stage of the process, and a reduction in the OH content of ~10 times was achieved [10], as illustrated in Fig. 4. It is also possible to obtain Cl_2 from $GeCl_4$ if a compensated collapse is attempted [18]. The fiber with loss spectrum shown by the upper curve in Fig. 4 contains ~0.25 parts in 10^6 of OH, whereas the OH peak at 1.39 μm in the lower curve amounts to ~1 dB/km, representing an OH level of ~30 parts in 10^9. The most important change is at 1.3 μm, which lies between the 1.39 μm overtone and the 1.25 μm combination band. The difference between these loss spectra is greater than can be attributed to OH alone since the two fibers were pulled under slightly different conditions.

The fluorine in the cladding has been used to cancel the refractive index rise due to P_2O_5 and also to produce large depressions in refractive index for *W* fiber, and therefore a wide range of fluorine deposition rates has been studied. The incorporation of F as a dopant in SiO_2 waveguides was described several years ago [19] but its use in the MCVD process and in ultra-low-loss monomode fibers is a relatively recent development [8]. In this work CCl_2F_2 (freon 12) has been used as the source of F since it was readily available in high purity form. It has been found that the incorporation of F into SiO_2 reduces the reaction rate in the MCVD process, and this is illustrated in Fig. 5(a). For fixed $SiCl_4 + O_2$ and $POCl_3 + O_2$ flow rates, increasing the flow of CCl_2F_2 from 0 to 160 ml/min depresses the relative deposition rate to 40 percent. The reasons for this are unclear but it is possible that volatile Si-F compounds are formed which are not easily incorporated into the glass structure. Fig. 5(b) shows how the refractive index of the deposited material diminishes with increasing CCl_2F_2 flow rate. The effect is not linear and it becomes increasingly difficult to achieve a large depression in refractive

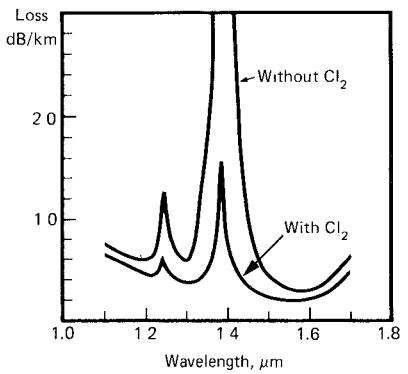

Fig. 4. The effect of Cl_2 drying during collapse of the substrate.

index by increasing the freon flow rate. The reduction in deposition efficiency for large flows means that CCl_2F_2 has limited usefulness since a large depression in refractive index requires significantly longer deposition time for a given size of preform than in the F-free case. However, the $POCl_3$ at normal flow rates generates a rise in refractive index of ~0.0006 over that of silica, and only a very low flow of CCl_2F_2 is necessary to compensate, which barely affects the reaction rate. The concentration of $POCl_3$ in the vapor stream (for constant $SiCl_4 + O_2$ and CCl_2F_2 flow rates) appears to have less influence on the refractive index of the glass than would be expected, as shown in Fig. 5(c). Curve (i) is a linear fit to the points shown, with the refractive index rising by 0.00033 for 160 ml/min $POCl_3 + O_2$ flow rate. However, calibration of the effect of $POCl_3$ in the absence of CCl_2F_2 gives a gradient shown as the dashed line (ii), an increase of 0.0008. As the $POCl_3$ concentration is increased the deposition temperature is reduced to maintain optimum deposition of the glassy layers, and therefore these data suggest that the incorporation of F may be favored by a low process temperature, the difference between curves (i) and (ii) representing a higher F content at higher P_2O_5 concentrations. This hypothesis is currently awaiting further experimental confirmation.

The fibers were drawn using a graphite resistance furnace and coated with thermally cured silicone polymers. Fiber diameter variations were normally $< \pm 1$ μm, and exceptionally ± 0.3 μm. A forward scattering technique, employing a HeNe laser to project diffraction patterns of the coated fiber onto screens, was used to monitor the concentricity of the coating. Fiber drawing speeds were in the range 10-30 m/min, with 20 m/min being typical. Some preforms were sleeved with additional WG tubes to increase the volume of glass, with a corresponding adjustment in the volume of deposited material to achieve the correct aspect ratio, which enabled long continuous pieces (up to 30 km) of fiber to be drawn.

III. The Design of "Matched Cladding" Fiber

Recent progress in understanding the interplay between monomode fiber design and performance [5] allows fresh insight into the fiber options which are available for designing long distance monomode systems. The wavelength of zero dispersion λ_0 can be adjusted over a wide range, which means that the fiber options can vary between the extremes of large core and small δn to small core and large δn. Because of the shape of the refractive index profile in real fibers, in particular the central dip, it is desirable to discuss the fiber design in terms of an equivalent step index profile (ESI) as well as peak

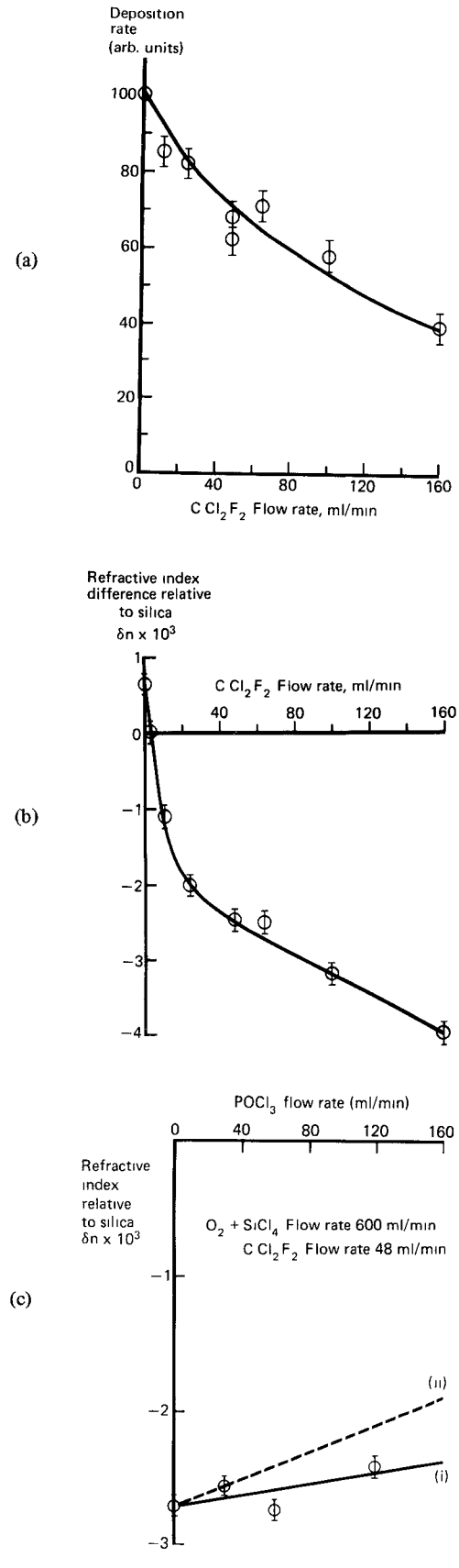

Fig. 5. (a) Deposition rate of P_2O_5 +F doped SiO_2 as a function of CCl_2F_2 flow rate. O_2 + $SiCl_4$ flow rate is 600 ml/min and $POCl_3$ is 120 ml/min. (b) Refractive index difference δn between P_2O_5 +F doped SiO_2 and pure SiO_2 as a function of CCl_2F_2 flow rate. Other flows are as above. (c) Refractive index difference δn between P_2O_5 +F doped SiO_2 and pure SiO_2 as a function of $POCl_3$ +O_2 flow rate at fixed CCl_2F_2 flow rate. (i) Line fitted to results Φ. (ii) Slope that would be obtained with no CCl_2F_2 present.

δn (maximum core refractive index-cladding refractive index) [20], [21]. In this work it has been found that on the average $\delta n(\text{ESI}) \approx 0.7\delta n(\text{peak})$. In Fig. 6 we have plotted δn(ESI) against core diameter $2a$. A given point (δn, $2a$) then represents a certain value of V, and loci are drawn for $V = 2.4$ at $\lambda = 1.0$ and 1.2 μm. The region enclosed by these two lines, therefore, represents the conditions for the fiber to be monomode at both 1.3 and 1.55 μm ("dual window"). Also shown as dotted curves are lines of constant λ_0 [22], [23]. The combination of λ_{co} and λ_0 uniquely defines which fiber design should be chosen for a given system performance.

We have arbitrarily identified four regions in this diagram, representing four classes of fiber *A*-*D*. Type *A*, with large core, small δn, has λ_0 close to 1.3 μm but shows a strong tendency to bending losses for $V < 1.9$. Fibers of type *B* show more stable guidance, but λ_0 lies in the region 1.31-1.35 μm, giving slightly inferior system performance at 1.3 μm. Type *D* fiber represents a design with $\lambda_0 \sim 1.55$ μm to coincide with the theoretical minimum loss, and while very stable guidance is achieved, constraints on fiber geometry and jointing techniques are more severe than for types *A* and *B* owing to the narrower mode field width [24]. An intermediate design *C* is a compromise between *B* and *D*, with equal dispersion (10 ps/km/nm) at 1.3 and 1.55 μm. The implications of the bandwidths of these fibers on possible system designs is illustrated in Fig. 7, assuming a source with 5 nm linewidth, and making simple assumptions for the conversion from dispersion to bandwidth. These curves were calculated from the materials dispersion data of Fleming [25] using the approximations of White and Nelson [26] with 2.3, 3.2, 5.6, and $10.2^m/_o$ GeO_2 in SiO_2. Second-order effects such as ellipticity and stress birefringence have been ignored, but a rigorous treatment of dispersion in monomode fibers has been presented by Marcuse and Lin [4]. Fig. 7 shows that while each type of fiber is capable of a very high bandwidth close to its λ_0, this falls by 1-2 orders of magnitude at wavelengths of $\lambda_0 \pm 0.1$ μm. However, type *B* fiber with $\lambda_0 = 1.33$ μm can carry a 30 km, 280 Mbit/s system even at 1.55 μm, which is better than high quality graded index multimode fiber operating at its optimum dispersion point.

We have yet to consider the attenuation levels which may be achieved in fibers *A*-*D*. Increasing the GeO_2 dopant concentration in the core of the fiber leads to increased loss from both scattering and absorption. The Rayleigh scattering is intrinsic to a given composition, but the absorption depends on the fiber fabrication conditions [5]. One way of minimizing the absorption loss is to decrease the fiber drawing temperature [5], but this may lead to problems with fiber strength. In Fig. 8 we illustrate the minimum loss and range of loss which may be expected as δn is increased. The lowest reported losses for type *A* fiber are 0.20 dB/km at 1.55 μm [2] and 0.37 dB/km at 1.3 μm [5]. For type *D*, <0.4 dB/km has been achieved at 1.55 μm by optimizing the drawing conditions [5], but the attenuation can increase rapidly at high drawing temperatures, as shown in Fig. 8. The corresponding loss minimum for *D* at 1.3 μm is 0.6 dB/km.

If we now combine the dispersion data with the loss data to obtain an overall systems performance, we can assess the full potential of the four classes of fiber. Type *A*, with $\lambda_{co} \sim 1.1$-1.2 μm, is suitable for systems operating at 1.3 μm, but be-

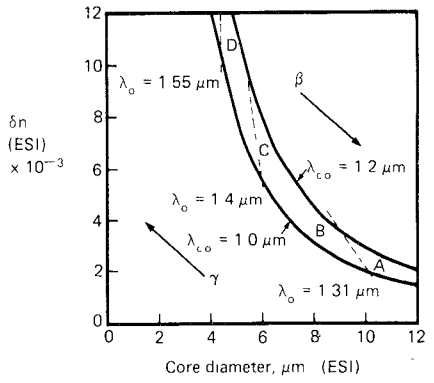

Fig. 6. Design diagram for matched cladding fiber. Solid lines give the cutoff conditions at 1.0 and 1.2 μm for the LP_{11} mode. Dashed lines define conditions for zero dispersion at 1.31, 1.4, and 1.55 μm. A: Weakly guiding fiber, suitable for 1.3 μm operation. B: Optimized dual-window fiber with low dispersion at 1.3 μm. C: Dual-window fiber with equal dispersion at 1.3 and 1.55 μm. D: dispersion-shifted fiber with $\lambda_0 \sim 1.55$ μm. β: Increasing bending loss susceptibility. γ: Increasing jointing loss susceptibility.

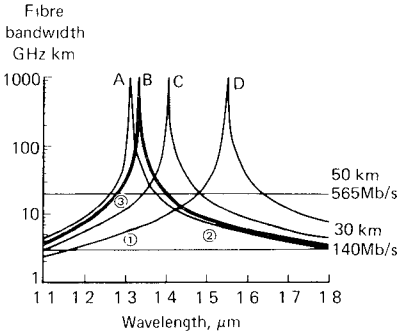

Fig. 7. Bandwidths of fiber types A–D as a function of wavelength assuming a source of 5 nm linewidth. ①, ②, and ③ show systems demonstrated on B type fiber. ①140 Mbits/s, 37 km, ②140 Mbits/s, 49 km, ③650 Mbits/s, 37.4 km.

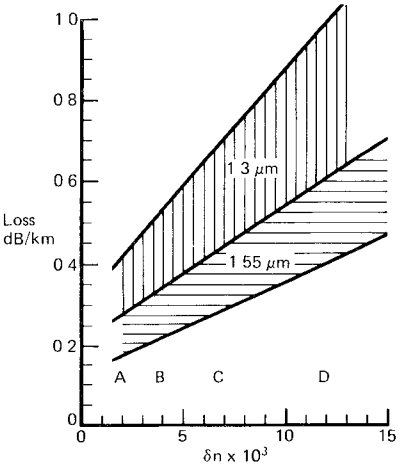

Fig. 8. The effect of changing fiber design on attenuation. The range of loss shown at a given value of δn allows for varying fiber fabrication conditions (e.g., drawing temperature).

comes bandwidth-limited at 1.55 μm, and more importantly, is too prone to bending losses for practical applications even though the fundamental loss is very low. Type B compromises bandwidth slightly at 1.3 μm, but offers low loss and stable guidance in the 1.3 and 1.55 μm windows but with limited bandwidth at 1.55 μm. Both loss and bandwidth of type C are sacrificed to offer equal but relatively poor dispersion performance in both windows, while incurring a loss penalty of ~ 1.5 times compared with types A and B. Therefore, this design seems to have no benefits over others. Although type D offers very high bandwidth at 1.55 μm, where it has lowest loss, the loss penalties which appear intrinsic to type D mean that its usefulness is questionable. At present, type D systems will become loss-limited long before they become bandwidth-limited. The recent development of injection-locked lasers offering narrow linewidths ($\ll$1 nm) [27] calls into question the philosophy of dispersion shifting, and in the future it may be more sensible to pursue designs close to type B unless the high peak power from such devices gives rise to stimulated Brillouin scattering [28].

If operation at only one wavelength were required, "single window" fiber designs would offer more stable performance with less severe constraints on fabrication. For 1.3 μm, type A, operating close to the LP_{11} cutoff, offers lowest loss and dispersion. At 1.55 μm, type A' (not shown in Fig. 6, but with slightly increased δn or a) with $\lambda_{co} \sim 1.4$ μm to minimize bending sensitivity, would give the lowest loss and could be used with narrow linewidth devices to avoid dispersion limitations. The 1.3 μm window is more sensitive to the OH content of the fiber than the 1.55 μm window and single-window fiber operation at 1.55 μm will probably be the ultimate choice when narrow linewidth devices become generally available, or if wavelength multiplexing is required.

The design criteria discussed above also apply to depressed cladding fiber, provided that the diameter of the depression is wide enough to approximate to an infinite cladding. This will be discussed in more detail in Section V.

IV. Results and Discussion for Matched Cladding Fiber

From the preceding discussion it may be concluded that fibers of type A, B, and D are the most interesting from the systems point of view and results will be reported for all three types, with emphasis on B. If "dual window" fiber capable of high performance at 1.3 and 1.55 μm is considered, it is interesting to investigate the limits of operation with fibers having low values of δn to see under what conditions bending losses become a problem as V is reduced. Fig. 9 shows the loss spectra for three fibers with nominally the same δn(peak) $\sim$ 0.0045, as pulled on drums 220 mm in diameter at low tension ($<$25 g). Bending losses become significant in these fibers when $V < 1.7$, and fibers with δn(peak) < 0.0045 were found to be progressively more sensitive at higher values of V. Those with δn(peak) > 0.0045 were relatively insensitive for $V >$ 1.6, i.e., fibers with $\lambda_{co}(LP_{11})$ in the region 1.1-1.2 μm showed stable guidance at 1.55 μm for the higher range of δn.

As a means of investigating the performance of this type of fiber, a series of 10 consecutive preforms was made with $0.0045 < \delta n$(peak) < 0.0055, using deposition tubes 20 X 16 mm, with a cladding deposition rate of 0.25 g/min. These gave fibers of length 6-7 km, with the range of attenuation shown in Fig. 10(a). It is well known that the end of the preform at which the vapor stream is introduced suffers from gradients of thickness and composition of the layers owing to the thermo-

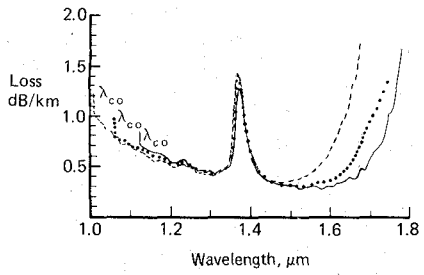

Fig. 9. Transmission windows of three fibers with δn(peak) = 0.0045, showing bending losses at $V \sim 1.6$. λ_{co} is the LP_{11} cutoff wavelength for each fiber.

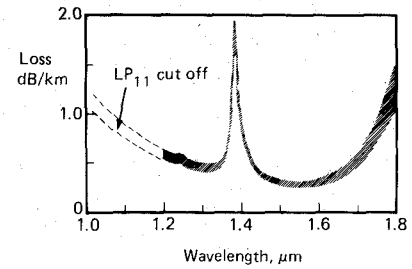

(a)

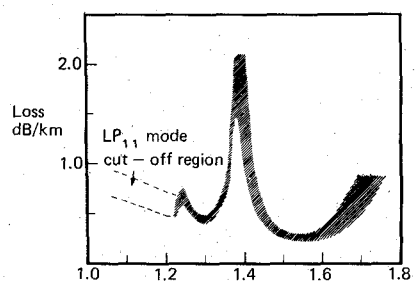

(b)

Fig. 10. (a) Range of loss measured for each fiber from 10 consecutive preforms (64 km fiber). Deposition tube size was 20 × 16 mm and cladding deposition rate 0.25 g/min. (b) Range of loss measured for fibers from six preforms (66 km fiber). Tube size was 25 × 19 mm, deposition rate 0.5 g/min.

phoretic deposition process not having reached equilibrium. The length of this "input taper" is a function of the deposition conditions (e.g., vapor flow rates, water cooling of the substrate tube [16]) and for the preforms described above this region was discarded before the fiber was drawn. Subsequently, a further six preforms were made on a new deposition apparatus at a rate of 0.5 g/min in tubes 25 × 19 mm, and the range of loss for the fibers drawn from these is shown in Fig. 10(b). These fibers averaged 11 km in length. It is clear that the attenuation levels are well controlled in both series, with mean loss figures being almost identical. More recent preforms with 0.75 g/min deposition rate have also given identical fiber losses, indicating that the loss can be maintained over a wide range of deposition rates. The OH peaks at 1.39 μm in the second series are more variable than the first but this was traced to an impure source of Cl_2 which was used for the drying procedure. The OH content of subsequent fibers made on the same equipment was consistently the same as in the first series. The LP_{11} cutoffs for these fibers lay in the wavelength range 1.0-1.25 μm. Loss histograms for both series are

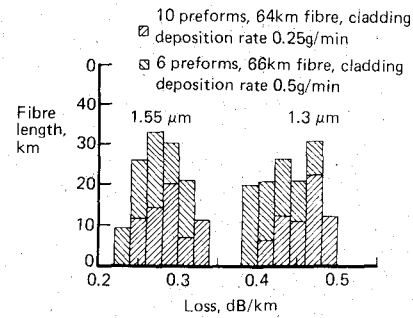

Fig. 11. Histogram of losses at 1.3 and 1.55 μm for the fibers in Fig. 10.

shown for 1.3 and 1.55 μm in Fig. 11. The total fiber length amounts to 130 km, and the mean losses are 0.44 and 0.28 dB/km, respectively.

Another parameter of interest is the joint loss which may be expected in any fiber design. For fusion jointing in which fibers are aligned relative to their outer surfaces, good core concentricity is vital if low joint losses are to be achieved [24]. The concentricity error is defined as the length of the radius vector between the center of the total fiber cross section and the center of the core. In Fig. 12 a histogram of core eccentricities is shown for the two series of fibers. The data refer to the ends of the original lengths of fiber, but the fibers from the first series were subsequently cut into lengths of 2.2 km for packaging and cabling. The fiber ends from the middle sections of the preforms showed more consistent concentricity than the extreme ends. The average eccentricity of the ends of the 2.2 km sections was < 0.4 μm, which indicates a mean loss of < 0.1 dB per joint due to core misalignment [29]. As measured eccentricities in the fibers do not correlate with variations in thickness of the walls of the deposition tubes (siding), especially in the second series, deformation of the substrate during deposition may contribute to the core eccentricity. None of the preforms in this exercise was sleeved, and in sleeved preforms it has been found that the core eccentricity tends to be more variable. This may result from eccentricity of the preform in the sleeving tube leading to asymmetrical collapse in the fiber drawing process.

Dispersion results for some of the above fibers have been obtained and in general they agree well with the theoretical predictions. Details of these measurements have been published by White *et al.* [30]. No strong evidence of pulse broadening due to ellipticity or stress birefringence has been observed.

The exercise described above has been most useful in highlighting the manufacturing tolerances required to meet given design criteria, and shows that tight control over the core dopant level and the resulting δn is necessary. The value of δn (peak) should not fall below ~ 0.0045 in dual-window fiber to ensure low sensitivity to bending, while deviations to higher values lead to excess loss. Work is continuing to reduce preform end variations (input taper) by computer control of the deposition process (e.g., ramping lathe traverse functions in an attempt to cancel the input taper). Consistent loss and dispersion performance can now be attained in type *B* fiber, and a typical result is shown as curve *B* in Fig. 13 for a 9.2 km length. The loss minima are 0.38 dB/km at 1.3 μm and 0.22 dB/km at 1.55 μm. By drawing *D* type fiber under suitable conditions, losses of 0.6 and 0.37 dB/km have been obtained

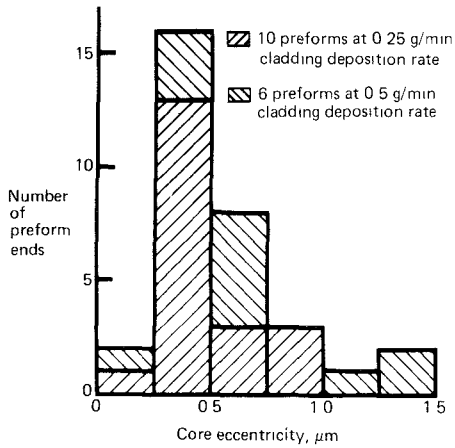

Fig. 12. Histogram of core eccentricities for the fibers in Fig. 10.

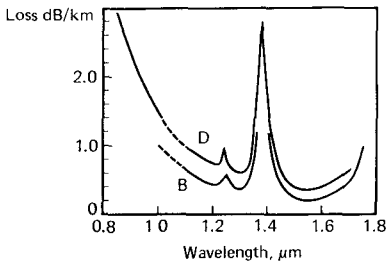

Fig. 13. Loss spectra for (B) 9.2 km of fiber with δn(peak) = 0.004 and (D) 2 km of fiber with δn(peak) = 0.013.

at 1.3 and 1.55 μm, respectively, as shown by curve D in Fig. 13.

The successful fabrication of B type fiber with low loss over a range of deposition rates has led to attempts at making longer lengths by sleeving large preforms, and over 30 km has been drawn in one piece from a preform made in a 25 X 19 mm substrate tube, sleeved with a tube of the same dimensions. The loss of this length of fiber was measured as 0.44 dB/km at 1.3 μm and 0.31 dB/km at 1.55 μm. There was evidence of additional bending loss at longer wavelengths, probably due to the multilayer winding of such a long length onto a drum 320 mm in diameter, combined with the LP_{11} cutoff lying at <1.1 μm, giving $V \sim 1.6$ at 1.6 μm. The core eccentricities in this fiber were 0.9 and 0.5 μm at the ends, which compare favorably with the results shown in Fig. 12 for the larger preforms.

For a laboratory systems trial, a 28.2 km length of this fiber (remaining after samples had been cut from both ends of the original length) was jointed to the 9.2 km length referred to in Fig. 13, producing a total of 37.4 km. The spectral loss of this link was measured using a lamp/monochromator technique with a low noise Ge detector cooled to 77 K, and the result is shown in Fig. 14. The jointed link showed a total loss of 0.45 dB/km at 1.3 μm and 0.29 dB/km at 1.55 μm, and has been used by Hooper and co-workers [31] to demonstrate a 650 Mbits/s system. The main features of the system are summarized in Table I, which also includes details of two earlier systems working at 140 Mbits/s [32]. The performance of these systems is represented in Fig. 7 by: ① 140 Mbits/s, 37 km at 1.3 μm; ② 140 Mbits/s, 49 km at 1.5 μm, and ③ 650 Mbits/s, 37.4 km at 1.3 μm. Although these results show the feasibility of using type B fiber at 1.3 μm for high capacity

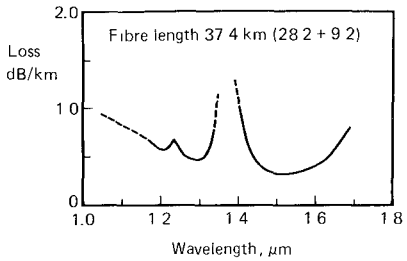

Fig. 14. Spectral loss of 37.4 km jointed link of B type fiber measured using Ge detector cooled to 77 K with lamp/monochromator source.

TABLE I

System	①	②	③
Wavelength (μm)	1.31	1.51	1.3
Length (km)	37	49	37.4
Bit rate (Mb/s)	140	140	650
Launch power (dBm)	-11	-15.4	-10
Fibre loss at 1.3μm (dB)	28		16.5
Fibre loss at 1.55μm (dB)		24	11
System margin (dB)	3.3	3.2	2

systems over 30-50 km in the laboratory, for practical systems cabling and jointing losses and systems margins must be considered. Future improvements in launch power and receiver sensitivity may allow similar performance to be attained in practical systems. The successful development of injection-locked lasers may also lead to equal or better performance with the same fiber design in the 1.55 μm window.

V. Depressed Cladding Fiber

In previous papers an alternative monomode fiber structure was proposed [5], [33] in which the refractive index (n_2) of the deposited cladding is below that of both the core (n_1) and the substrate (n_3). A typical preform profile for a depressed cladding (DC) fiber with (n_1-n_2) equivalent to type B is shown in Fig. 15(a). A schematic profile which defines the refractive index levels and the radii of the core and depressed regions is shown in Fig. 15(b). The refractive index depression relative to pure SiO_2 is 0.0025, but as discussed in Section II, depressions of up to 0.004 have been achieved with the materials and apparatus described.

W fibers were proposed some years ago [6] as a means of obtaining: 1) tight mode confinement to the core, 2) a reduction in waveguide dispersion, and 3) less sensitivity to bending losses compared with the equivalent matched cladding (MC) fibers. To obtain these benefits, the thickness of the depressed region

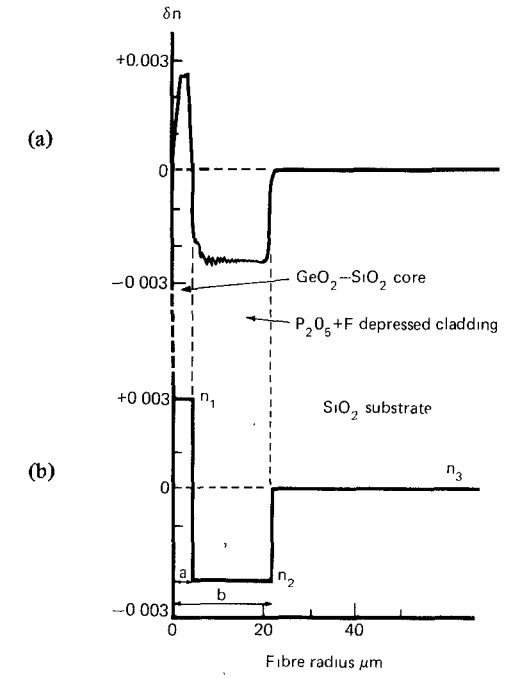

Fig. 15. (a) Refractive index profile of "*B* equivalent" depressed cladding preform. (b) Schematic profile defining core radius a, depressed cladding radius b, and refractive index levels n_1, n_2, and n_3.

$(b-a)$ should be $< a$, and thus a typical monomode W fiber would require further cladding material of index n_3 to be deposited at radii $> 2a$. The current DC fiber is designed with $b > 5a$ (infinite cladding approximation) as a means of decreasing the concentration of GeO_2 in the core for any required total value of $(n_1 - n_2)$, consequently reducing the GeO_2 dependent scattering and absorption losses which were described earlier. Fig. 16 demonstrates a low loss DC fiber of the type shown in Fig. 15. The total δn is as for type B and the attenuation is 0.37 dB/km at 1.3 μm and 0.21 dB/km at 1.55 μm. In Fig. 16 the LP_{11} cutoff appears approximately at the expected position for the equivalent MC fiber (i.e., $\delta n(\text{peak}) = 0.005$, $2a = 8.5$ μm), but the loss for $V < 1.8$ ($\lambda > 1.6$ μm) rises more sharply than is normally experienced in those MC fibers which are sensitive to bending losses (c.f. Fig. 9). This could be explained in terms of the perturbation to the tail of the guided mode field caused by the higher index substrate n_3, since reference to Fig. 2 shows that in the infinite cladding approximation, $\sim 10^{-3}$ of the power still remains at $b/a > 5$. As V decreases at longer wavelengths this fraction rapidly becomes more significant.

However, if the W fiber theory of Kawakami and Nishida [6], [34], [35] is applied for large b/a, the behavior described above can be analyzed in a different way. First-order perturbation theory suggests that the mode cutoff wavelengths in W fiber are quite different from those in the MC equivalent, and λ_{co} depends on $(n_1 - n_3)$ rather than $(n_1 - n_2)$. The theory also predicts a cutoff for the fundamental (LP_{01}) mode. This leads to the estimate of λ_{co} (LP_{11}) ~ 0.7 μm and λ_{co} (LP_{01}) ~ 1.3 μm for the fiber in Fig. 16. When $\lambda > \lambda_{co}$ the mode is leaky, and it becomes very lossy at the wavelength predicted for the cutoff of the equivalent MC fiber. This is illustrated in [34, Fig. 3]. Therefore, it could be argued that the LP_{11} mode

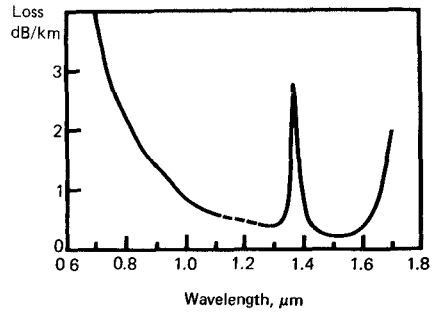

Fig. 16. Loss spectrum for 2.3 km of "*B* equivalent" depressed cladding fiber. Dashed line shows apparent LP_{11} cutoff.

for the fiber shown in Fig. 16 has actually cutoff at 0.7 μm, but continues to propagate as a leaky mode until $\lambda \sim 1.2$ μm. Since b/a is relatively large, the attenuation constant for the mode in the leaky region is very small for sufficiently large V [34, Fig. 4], with the result that the DC fiber appears to behave as the equivalent MC fiber. Similarly, if the LP_{01} mode cuts off at ~ 1.3 μm but continues to propagate as a leaky mode with very low attenuation constant, the fiber has low loss for sufficiently large V, until the attenuation constant becomes significant as V decreases, causing a rapid increase in loss and an apparent cutoff. The attenuation constants for the modes in the leaky wave region are functions of b/a, and therefore it is probable that the wavelength of the apparent LP_{01} cutoff can be moved to longer wavelengths by choosing sufficiently large b/a.

The reduction in GeO_2 concentration in DC fiber compared with MC fiber means that the material dispersion zero in DC fiber will move to shorter wavelengths. Consequently, for type A and B fibers λ_0 will lie about 15 nm closer to 1.3 μm than for the MC equivalent, which is an advantage for 1.3 μm operation. However, in type D equivalent MC fiber the reduction in λ_0 means that waveguide dispersion will have to be increased to maintain $\lambda_0 = 1.55$ μm. This is a disadvantage since the core diameter would have to be reduced, resulting in a higher probability of poor jointing performance.

In the leaky mode wavelength region it might be supposed that the LP_{01} mode would be very sensitive to perturbations in the fiber (e.g., microbending), but the fiber shown in Fig. 16 has been packaged by the loose tube technique with no increase in loss [36]. However, the stability of DC fiber in very long lengths requires further investigation since variations in a, b, and δn along the fiber may cause the long wavelength cutoff to shift to shorter wavelengths. This is the subject of continuing study and will be reported in a later publication. We have demonstrated here that ultra-low-loss DC fiber can be fabricated and propagation in the leaky mode wavelength range appears to be stable provided b/a is sufficiently large.

VI. Summary

In this paper we have considered a range of monomode fiber designs, and reported results for two classes of fiber: matched cladding and depressed cladding. The fabrication requirements have been discussed with reference to the materials which are suitable for making low loss monomode fiber for use in the wavelength region 1.0-1.8 μm, and an attempt has been made

to arrive at a balance between good optical performance and ease of fabrication.

The compromises involved in optimizing dispersion and attenuation simultaneously have been considered and the fiber design has been refined in an attempt to achieve these aims. We have demonstrated results for MC fiber which show that ultra-low-loss can be achieved in fiber designs for 1.3 μm. The results are consistent over a range of deposition rates and over continuous length up to 30 km. Fiber dimensions and concentricity have also been controlled to fine limits, enabling reproducible jointing results to be achieved. System demonstrations using this fiber are also mentioned, confirming that design criteria have been met. Ultralow attenuation has also been demonstrated in DC fiber, and its propagation characteristics have been compared with predictions from W fiber theory. In MC fiber the fundamental mode has no cutoff but the loss can increase at small values of V due to bending effects, whereas according to W fiber theory, the LP_{01} mode has a finite cutoff wavelength above which the mode is leaky with an attenuation constant which depends on b/a. Further experimental work on DC fiber is necessary to confirm this analysis.

Acknowledgment

The authors gratefully acknowledge the continued excellent technical assistance of D. A. Colthorpe and W. A. Merlo, and also M. C. Brierley, H. P. Girdlestone, S. Hornung, D. McCartney, C. Millar, B. P. Nelson, J. Stern, K. I. White, and J. V. Wright for assistance at various stages of this work. They would also like to thank the Director of British Telecom Research Laboratories for permission to publish this work.

References

[1] J. B. MacChesney, "Materials and processes for preform fabrication–Modified chemical vapour deposition and plasma chemical deposition," *Proc. IEEE*, vol. 68, pp. 1181-1184, 1980.

[2] T. Miya, Y. Terunuma, T. Hosaka, and T. Miyashita, "Ultimate low loss single-mode fibre at 1.55 μm," *Electron. Lett.*, vol. 15, pp. 106-108, 1979.

[3] I. P Kaminow, D. Marcuse, and H. M. Presby, "Multimode fibre bandwidth: Theory and practice," *Proc. IEEE*, vol. 68, pp. 1209-1213, 1980.

[4] D. Marcuse and C. Lin, "Low dispersion single-mode fibre transmission–The question of practical versus theoretical maximum transmission bandwidth," *IEEE J. Quantum Electron.*, vol. QE-17, pp. 869-878, June 1981.

[5] B. J. Ainslie, K. J. Beales, C. R. Day, and J. D. Rush, "Interplay of design parameters and fabrication conditions on the performance of monomode fibre made by MCVD," *IEEE J. Quantum Electron.*, vol. QE-17, pp. 854-857, June 1981.

[6] S. Kawakami and S. Nishida, "Characteristics of a doubly clad optical fibre with a low index inner cladding," *IEEE J. Quantum Electron.*, vol. QE-10, pp. 879-887, 1974.

[7] M. Okada, M. Kawachi, and A. Kawana, "Improved chemical vapour deposition method for long length optical fibre," *Electron. Lett.*, vol. 14, pp. 89-91, 1978.

[8] B. J. Ainslie, C. R. Day, P. W. France, K. J. Beales, and G R. Newns, "Preparation of long lengths of ultra low loss single mode fibre," *Electron. Lett.*, vol. 15, pp. 411-413, 1979.

[9] H. Murata and N. Inagaki, "Low loss single-mode fibre development and splicing research in Japan," *IEEE J. Quantum Electron.*, vol. QE-17, pp. 835-849, June 1981.

[10] B. J. Ainslie, C. R. Day, J. D. Rush, and K. J. Beales, "Optimised structure for preparing long ultra-low-loss single mode fibres," *Electron. Lett.*, vol. 16, pp. 692-693, 1980.

[11] T. Edahiro, M. Horiguchi, K. Chida, and Y. Ohmori, "Spectral loss characteristics of GeO_2-P_2O_5-doped silica graded-index fibres in long wavelength band," *Electron. Lett.*, vol. 15, pp. 274-275, 1979.

[12] H. Osanai, T. Shioda, T. Moriyama, S. Araki, M. Horiguchi, T. Izawa, and H. Takata, "Effects of dopants on transmission loss of low OH content optical fibres," *Electron. Lett.*, vol. 12, pp. 549-550, 1976.

[13] J. Irven, "Long wavelength performance of $SiO_2/GeO_2/P_2O_5$ core fibres with different P_2O_5 levels," *Electron. Lett.*, vol. 17, pp. 2-3, 1981.

[14] D. Gloge, "Weakly guiding fibres," *Appl. Opt.*, vol. 10, pp. 2252-2258, 1971.

[15] York Technology, Winchester, U.K. Original work by I. Sasaki, D. N. Payne, and M. J. Adams, "Measurement of refractive index profiles in optical fibre preforms by spatial filtering technique," *Electron. Lett.*, vol. 16, pp. 219-221, 1980.

[16] T. J. Miller and D. A. Nicol, "Compositional variations in individual modified chemical vapour layers prior to consolidation," in *Proc. 3rd Int. Conf. Integrated Opt. and Opt. Fibre Commun.*, San Francisco, CA, Apr. 1981, paper WD1.

[17] J. Irven and A. P. Harrison, "Single mode and multimode fibres Co-doped with fluorine," in *Proc. 3rd Int. Conf. Integrated Opt. and Opt. Fibre Commun.*, San Francisco, CA, Apr. 1981, paper TuC4.

[18] A. D. Pearson, "Hydroxyl contamination of optical fibres and its control in the MCVD process," in *Proc. 6th European Conf. Opt. Commun.*, York, U.K., Sept. 1980, IEE Conf. Pub. 190, pp. 22-25.

[19] A. Muhlich, K. Rau, F. Simmat, and N. Treber, "New doped synthetic fused silica as bulk material for optical fibres," presented at 1st European Conf. on Opt. Fibre Commun., London, England, Sept. 1975, post-deadline paper.

[20] H. Matsumura and T. Suganuma, "Normalisation of single-mode fibres having an arbitrary index profile," *Appl. Opt.*, vol. 19, pp. 3151-3158, 1980.

[21] C. A. Millar, "Direct method of determining equivalent step index profiles for monomode fibres," *Electron. Lett.*, vol. 17, pp. 458-460, 1981.

[22] H. Tsuchiya and N. Imoto, "Dispersion-free single-mode fibre in 1.5μm wavelength region," *Electron. Lett.*, vol. 15, pp. 476-478, 1979.

[23] T. Kimura, "Single mode digital transmission technology," *Proc. IEEE*, vol. 68, pp. 1263-1268, 1980.

[24] D. Marcuse, "Loss analysis of single-mode fibre splices," *Bell Syst. Tech. J.*, vol. 56, pp. 703-718, 1977.

[25] J. W. Fleming, "Material dispersion in light guide glasses," *Electron. Lett.*, vol. 14, pp. 326-328, 1978.

[26] K. I. White and B. P. Nelson, "Zero total dispersion in step index monomode fibres at 1.30 and 1.55 μm," *Electron. Lett.*, vol. 15, pp. 396-397, 1979.

[27] D. J. Malyon, D. W. Smith, and R. W. Berry, "Spectrum stablised laser transmitter," in *Proc. 3rd Int. Conf. Integrated Opt. and Opt. Fibre Commun.*, San Francisco, CA, Apr. 1981, paper ME5.

[28] N. Uesugi, M. Ikeda, and Y. Sasaki, "Maximum single frequency input power in a long optical fibre determined by stimulated Brillouin scattering," *Electron. Lett.*, vol. 17, pp. 379-380, 1980.

[29] D. B. Payne and D. J. McCartney, "Splicing and connectors for single mode fibres," in *Proc. Int. Conf. Commun.*, Denver, CO, June 14-18, 1981, vol. 2, pp. 27.6.1-27.6.5.

[30] K. I. White, S. Hornung, J. V. Wright, B. P. Nelson, and M. C. Brierley, "Characterization of single mode optical fibres," *Radio Electron. Eng.*, vol. 51, pp. 385-391, 1981.

[31] R. C. Hooper and B. R. White, unpublished.

[32] R. C. Hooper, D. R. Smith, and B. R. White, "Long repeater span monomode optical systems," in *Dig. Colloquim Opt. Fibre Syst.–Present and Future*, IEE, London, England, May 1981, IEE Dig. no. 1981/53.

[33] B. J. Ainslie, K. J. Beales, C. R. Day, and J. D. Rush, "Design and fabrication of monomode fibres for long wavelength operation," in *Proc. 3rd Int. Conf. Integrated Opt. and Opt. Fibre Commun.*, San Francisco, CA, Apr. 1981, paper TuC3.

[34] S. Kawakami and S. Nishida, "Perturbation theory of a doubly clad optical fibre with a low index inner cladding," *IEEE J. Quantum Electron.*, vol. QE-11, pp. 130-138, 1975.

[35] S. Kawakami, S. Nishida, and M. Sumi, "Transmission characteristics of W-type optical fibres," *Proc. Inst. Elec. Eng.*, vol. 123, pp. 586-590, 1976.

[36] S. Hornung and M. H. Reeve, private communication.

B. James Ainslie received the B.Sc. degree in chemistry from Queen Mary College, University of London, London, England, in 1969.

He is presently with British Telecom Research Laboratories, Ipswich, Suffolk, England. He has worked on the materials aspects of thin films for silicon microtechnology and has been involved in various projects associated with low-loss optical fiber materials. Since 1978 he has been responsible for the development of preform fabrication by the MCVD technique.

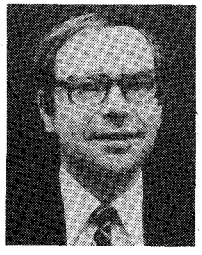

Keith J. Beales received the B.Sc. and Ph.D. degrees in chemistry from Nottingham University, Nottingham, England, in 1962 and 1965, respectively.

After completing a Post-Doctoral Fellowship at Nottingham University, he joined the British Post Office in 1966, and worked on materials aspects of silicon microtechnology and then on calcogenide switching glasses. In 1972 he transferred to work on optical fibers. Since 1979 he has been Section Head at British Telecom Research Laboratories, Ipswich, Suffolk, England. His responsibilities now include research into optical fibers prepared by MCVD and double crucible methods.

Clive R. Day received the B.Sc. degree in physics from the University of Wales, in 1966, and the D.Phil. degree in low temperature solid-state physics from Clarendon Laboratory, Oxford University, Oxford, England, in 1971.

In 1970 he joined the British Post Office to work in the optical fiber project. Presently, he is Group Head at British Telecom Research Laboratories, Ipswich, Suffolk, England, where he is responsible for research into single-mode fibers produced by the MCVD technique.

James D. Rush received the B.Sc. and Ph.D. degrees in physics from Liverpool University, Liverpool, England, in 1974 and 1978, respectively. His post-graduate and post-doctoral research work included Mossbauer spectroscopic studies of magnetic alloys and iron-containing proteins.

He joined British Telecom Research Laboratories, Ipswich, Suffolk, England, in 1979 and is a member of a group studying single-mode fibers produced by the MCVD method.